Reply to Referee #1 (Dr. D. Baumgardner)

Thank you very much for your reviewing our manuscript and providing us valuable comments and suggestions.

A single particle optical spectrometer, the CPS, is described for deployment on radiosondes that will count cloud particles and distinguish water droplets from ice crystals. The design is based on a commercial sensor that measures light scattered from aerosol particles and claims to separate pollen from other types of particles using polarization.

In my opinion, this paper is a long way from publication because it is missing some essential components that would make it a useful contribution: 1) scientific value, 2) Error analysis, 3) calibration details and 4) references to other instruments that measure the polarization state of cloud particles.

1) Scientific value
The introduction discusses the importance of clouds and talks about existing balloon borne cloud sensors but nowhere in the manuscript is there a discussion of either how balloon borne sensors contribute to the science or, in particular, how the sensor described in the paper, the CPS, will provide anything useful to our understanding of clouds.

The weather balloon with a radiosonde is one of the major platforms for upper air sounding, measuring vertical profiles continuously from the surface up to the middle stratosphere in ~100 minutes. The radiosonde temperature and humidity measurements, including those from balloon-borne special hygrometers, have been well characterized by regular and special intercomparison campaigns (e.g. Nash et al., 2011; Vömel et al., 2016). The typical balloon ascent rate is ~5 m s^{-1}, which is much smaller than the speed of aircrafts, easing some of the technical challenges that aircraft instruments may face (e.g. shattering of ice crystals; Baumgardner et al., 2012). On the other hand, balloon instruments need to be disposable, operable with small batteries, and of small mass. These factors may result in technical challenges when developing balloon-borne cloud particle instruments. As described in Introduction, the masses of existing balloon-borne cloud particle instruments range from 1 to 6 kg except for COBALD whose mass is ~500 g. The CPS is a balloon-borne instrument with a small mass (~200 g) which is comparable to that of modern radiosondes, and thus is much more easily combined with a radiosonde to detect the “existence” of cloud particles. This may provide advances in understanding of cloud and water vapour processes because this gives us more opportunities to obtain a set of vertical profiles of temperature, humidity, and (existence of) cloud particles compared to the existing much heavier balloon-borne instruments. A combination of radiosonde temperature and humidity measurements with a ground-based or satellite particle remote-sensing measurements (as discussed in Section 3.4, for example) may be another way to obtain such a data set, but the measurement collocation is always an issue particularly for high-altitude cirrus clouds (e.g. Shibata et al., 2007). As a disposable instrument, there is limitation in number concentration measurements, though we propose a simple, partial correction algorithm and a simple algorithm to convert the number of count to number concentration. Furthermore, utilizing the polarization information, the CPS can distinguish between water, ice, and mixed phase cloud layers (i.e. for a group of particles; even for a single particle for particular conditions); more detailed explanation on this is given below.

Some of the authors of this paper are considering the following specific applications: subvisual cirrus cloud processes in the tropical tropopause layer (TTL) (e.g. Iwasaki et al., 2004, 2007; Fujiwara et al., 2009; Shibata et al., 2007, 2012; Inai et al., 2012); radiosonde relative humidity sensor validation during radiosonde intercomparison campaigns; applications for dropsonde systems (by modifying the CPS1) to observe precipitating clouds (e.g. in association with typhoons); applications for long-duration balloon systems flying in the UTLS; among others. We believe that other researchers would have more ideas to utilize this instrument.

References:

Baumgardner, D., Avallone, L., Bansemer, A., Borrmann, S., Brown, P., Bundke, U., Chuang, P. Y., Cziczo, D., Field, P., Gallagher, M., Gayet, J.-F., Heymsfield, A., Korolev, A., Krämer, M., McFarquhar, G., Mertes, S., Möhler, O., Lance, S., Lawson, P., Petters, M. D., Pratt, K., Roberts, G., Rogers, D., Stetzer, O., Stith, J., Strapp, W., Twohy, C., Wendisch, M.: In situ, airborne instrumentation: Addressing and solving measurement problems in ice clouds, Bull. Amer. Meteorol. Soc., 93 (2), ES29–ES34, doi:10.1175/BAMS-D-11-00123.1, 2012.

Fujiwara, M., Iwasaki, S., Shimizu, A., Inai, Y., Shiotani, M., Hasebe, F., Matsui, I., Sugimoto, N., Okamoto, H., Nishi, N., Hamada, A., Sakazaki, T., and Yoneyama, K.: Cirrus observations in the tropical tropopause layer over the western Pacific, J. Geophys. Res., 114, D09304, doi: 10.1029/2008JD011040, 2009.

Inai, Y., Shibata, T., Fujiwara, M., Hasebe, F., and Vömel, H.: High supersaturation inside cirrus in well-developed tropical tropopause layer over Indonesia, Geophysical Research Letters, 39, L20811, doi: 10.1029/2012GL053638, 2012.

Iwasaki, S., Tsushima, Y., Shirooka, R., Katsumata, M., Yoneyama, K., Matsui, I., Shimizu, A., Sugimoto, N., Kamei, A., Kuroiwa, H., Kumagai, H., and Okamoto, H.: Subvisual cirrus cloud observations using a 1064-nm lidar, a 95 GHz cloud radar, and radiosondes in the warm pool region, Geophys. Res. Lett., 31, L09103, doi:10.1029/2003GL019377, 2004.

Iwasaki, S., Maruyama, K., Hayashi, M., Ogino, S.-Y., Ishimoto, H., Tachibana, Y., Shimizu, A., Matsui, I., Sugimoto, N., Yamashita, K., Saga, K., Iwamoto, K., Kamiakito, Y., Chabangborn, A., Thana, B., Hashizume, M., Koike, T., and Oki, T.: Characteristics of aerosol and cloud particle size distributions in the tropical tropopause layer measured with optical particle counter and lidar, Atmos. Chem. Phys., 7, 3507–3518, doi:10.5194/acp-7-3507-2007, 2007.

Nash, J., Oakley, T., Vömel, H., and Li, W.: WMO Intercomparison of high quality radiosonde observing systems, Yangjiang, China, 12 July - 3 August 2010, World Meteorological Organization Instruments and Observing Methods, Report IOM-107, WMO/TD-No. 1580, available at https://www.wmo.int/pages/prog/www/IMOP/publications-IOM-series.html, 2011. [Last access: 19 August 2016.]

Shibata, T., Vömel, H., Hamdi, S., Kaloka, S., Hasebe, F., Fujiwara, M., and Shiotani, M.: Tropical cirrus clouds near cold point tropopause under ice supersaturated conditions observed by lidar and balloon-borne cryogenic frost point hygrometer, J. Geophys. Res., 112, D03210, doi:10.1029/2006JD007361, 2007.

Shibata, T., Hayashi, M., Naganuma, A., Hara, N., Hara, K., Hasebe, F., Shimizu, K., Komala, N., Inai, Y., Vömel, H., Hamdi, S., Iwasaki, S., Fujiwara, M., Shiotani, M., Ogino, S.-Y., and Nishi, N.: Cirrus cloud appearance in a volcanic aerosol layer around the tropical cold point tropopause over Biak, Indonesia, in January 2011, J. Geophys. Res., 117, D11209, doi:10.1029/2011JD017029, 2012.

Vömel, H., Naebert, T., Dirksen, R., and Sommer, M.: An update on the uncertainties of water vapor measurements using cryogenic frost point hygrometers, Atmos. Meas. Tech., 9, 3755-3768, doi:10.5194/amt-9-3755-2016, 2016.

Based on a number of statements made throughout the paper, I don’t think that the authors have a very strong knowledge of cloud physics. They refer to "dense clouds" as those with concentrations of 2 particles per centimeters cubed, the limit to their sensor’s measurement capability. This is only the case for some cirrus clouds but certainly not for any low to mid-level water or mixed phased clouds.

Hence, the 2 cm3 coincidence threshold really makes this sensor useful only for cirrus clouds and you don’t need a polarization detector to tell you that you are in all ice. This makes the CPS just a cloud detector with no useful information on the number concentration until it get high in the atmosphere.

We admit that this is one of the major limitations of the CPS1. The priority when we started the development of this instrument was placed in developing a very small-mass, disposable instrument easily combined with a radiosonde (see also above for the characteristics of the radiosonde sounding). However, the CPS can distinguish the cloud phase at least as a layer (i.e. for a group of particles), and the phase of a single particle under particular conditions (please see below for more explanation). Also, we have provided a simple, partial correction algorithm for the number of count and a conversion algorithm to number concentration.

In addition, the assumptions that are made about the difference between the polarization signal from water and ice are wrong. They state that the polarization by water droplets is nearly zero but if they do the calculations, they will discover that only at 180 degrees is this true. Water droplets will change the polarization state at angles less than 180 degrees and as a function of size. Hence, unless this bias is taken into account, the detection system as currently set up will classify some water drops as ice. This bias is clearly shown in Figs. 6a and 9a.

First, the laser device, scattering particle, and the two detectors are placed within the same plane (Figure 1), and the polarization of the incident light is parallel to this plane, as described in Section 2.1. (We will add this information also in the caption of Figure 1 of the revised manuscript.) In this case, the polarization of the scattered light also becomes parallel to the plane regardless the scattering angle. In practice, they are not exactly parallel because of the finite volume of the detection area. In the Mie scattering calculations in Appendix A, we have considered this effect by rotating the Stokes parameter.

Second, in the revised manuscript, we will add the following explanation on the factory calibration process:
The rough-surface particles of 30−40 μm diameter are the spores of the Lycopodium clavatum Linnaeus provided by the Association of Powder Process Industry and Engineering (APPIE), Japan. Other rough-surface particles may also work; the key point is that we use certain particles so that we can calibrate the two detectors after the instrument is fully assembled. The sensitivity of the two detectors are differently adjusted so that the calibration particles give zero DOP on average (using 251 particle data). Typically, detector #2 is about three times more sensitive than detector #1; this is consistent with the fact that the polarization plate used has 34−35 % transmittance.

Third, in Figure R1-1, we show the DOP distributions obtained from the standard spherical particle experiments described in Appendix A. The results for the 5−30 μm particles are quite similar to the flight results for water clouds shown in Figures 4a, 6a, and 9a, namely, being distributed mostly at 0.3−1. For the smallest, 2 μm particles, the distribution is longer tailed to smaller (and negative) DOP values. For the 60 and 100 μm particles, whose I_{55} value was often saturated (as described in Appendix A), the distribution still resembles those for the 5−30 μm particles although it is somewhat longer tailed to smaller (but positive) DOP values. Figure R1-1 and corresponding discussion will be placed at the end of Appendix A of the revised manuscript.

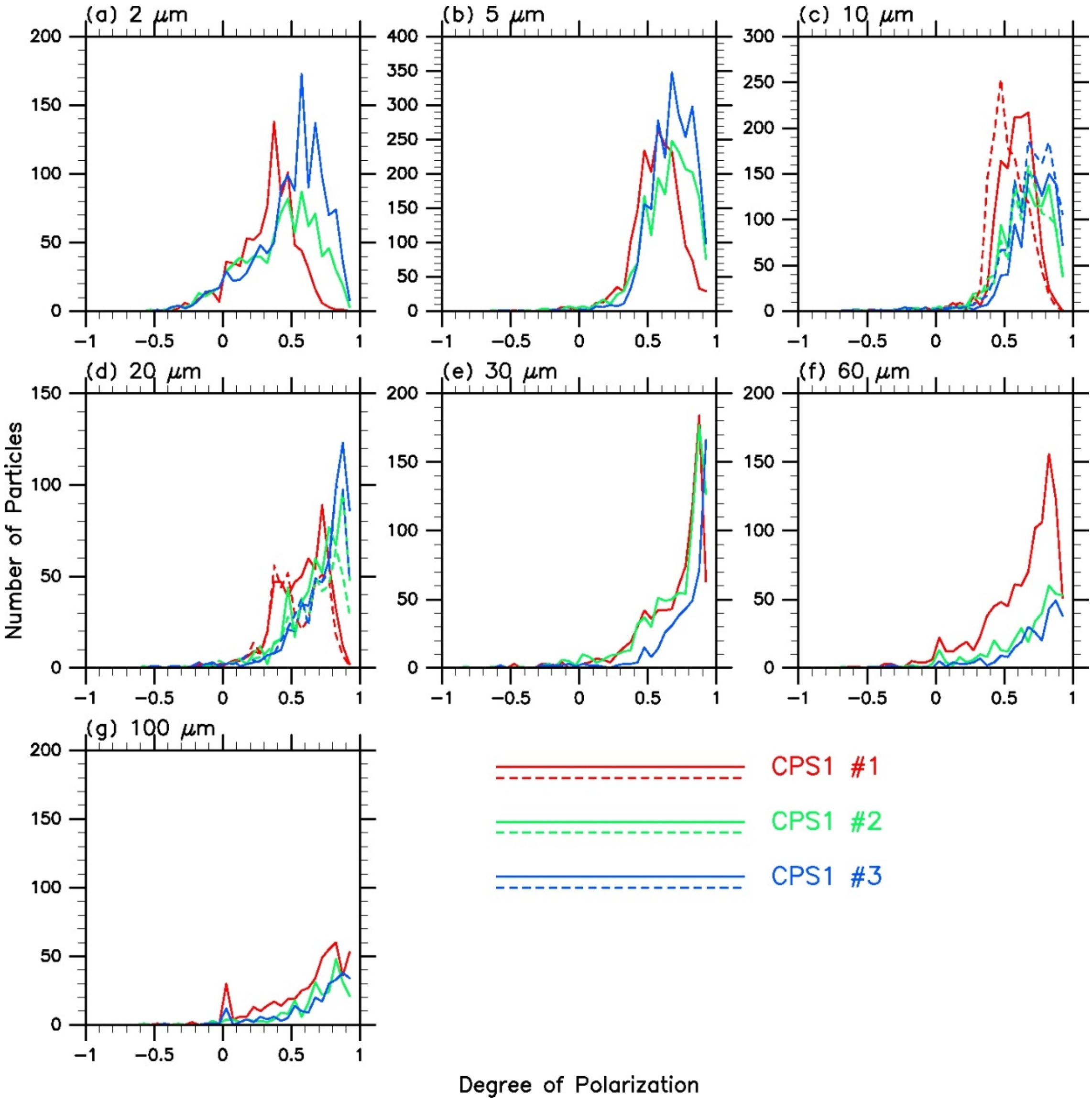

Figure R1-1. Frequency distributions of the degree of polarization (DOP) in 0.05 bins from the laboratory experiments using the standard spherical particles of (a) 2 µm, (b) 5 µm, (c) 10 µm , (d) 20 µm, (e) 30 µm , (f) 60 µm , and (g) 100 µm diameters. Red, green, and blue curves are for the CPS1 #1, #2, and #3 instruments, respectively. For the 10 µm and 20 µm particles (c and d), two sets of experiments on different days are expressed with solid and dotted curves.

Finally, in the revised manuscript, we will discuss the relationship between the DOP value and the phase of cloud particle more carefully (by referring to the above Figure R1-1 as well) as follows: When the DOP value is negative, the particle is ice. When the DOP value is positive but less than ~0.3, the particle is most likely ice. When the DOP value is more than ~0.3, the particle is water in many cases, but there is a chance that it is ice (because DOP can take values between −1 and +1 for ice particles; as shown in the flight results in the paper); for the final judgement, the DOP statistics of the cloud layer to which the particle is belong and the simultaneous temperature value should also be taken into account (as done in the paper).

2) Error analysis

No paper on measurement technique should be allowed publication without a serious error analysis and error propagation. The number "factor of 2" is given for concentration uncertainty but that is based on a very crude analysis. Given the many factors that affect the flow through the sample tube, the particle velocity can fluctuate much more than that.

The major factors that affect the flow speed within the detection area are the balloon ascent rate (~5 m s^{-1}), additional flow of within about +/−2 m s^{-1} due to the payload pendulum motions (depending on the length of the main string, payload configuration, and altitude), and the potential drag within the duct and around the detection area. Among them, it is considered that the balloon ascent rate determines the order of magnitude. As discussed in Section 2.3, we used hot-wire anemometers, with the uncertainty of +/−1 m s^{-1} (k = 2), to confirm this. In the revised manuscript, we will add a new appendix, Appendix B where we will show the results from a CPS with two hot-wire anemometers launched at Moriya at 17:11:47 LT on 23 November 2012 (see Figure R1-2). The two hot-wire anemometers were placed within a 6-cm long duct (with a similar inner cross section to that of the CPS's air inlet), near the two openings, and this duct was attached at the bottom side of a CPS. Thus, the anemometer #1 is located ~4 cm below the detection area, and the anemometer #2 is 9−10 cm below the detection area. Figure R1-2 compares the balloon ascent rate and the flow speed in the duct measured with two anemometers. From the surface up to ~10 km, the balloon ascent rate is 5−6 m s^{-1}, flow speed measured by the anemometer #1 is 4−5 m s^{-1}, and flow speed for #2 is 3−4 m s^{-1}, with increasing discrepancy between #1 and #2 at higher altitudes. Between 10 and 16 km, the balloon ascent rate is ~5 m s^{-1}, flow speed for #1 is ~4 m s^{-1}, and flow speed for #2 is 1−2 m s^{-1}. It is expected that the actual flow speed for #1 and #2 would not differ because of the same cross section of the air flow. However, the measurement results show that this was not the case. Possible reasons include the horizontal difference in the flow speed within the duct and in the location of the two anemometers (i.e. the anemometer #2 may have been located closer to the duct wall during the flight). Also, these anemometers might have had some directivity dependence, which had not been evaluated in the laboratory experiments. Considering the additional flow of up to 2 m s^{-1} due to the pendulum motions, assumption of a constant flow speed of 5 m s^{-1} with the uncertainty of a factor of ~2 (as the contribution from the flow-speed assumption) is not unreasonable.

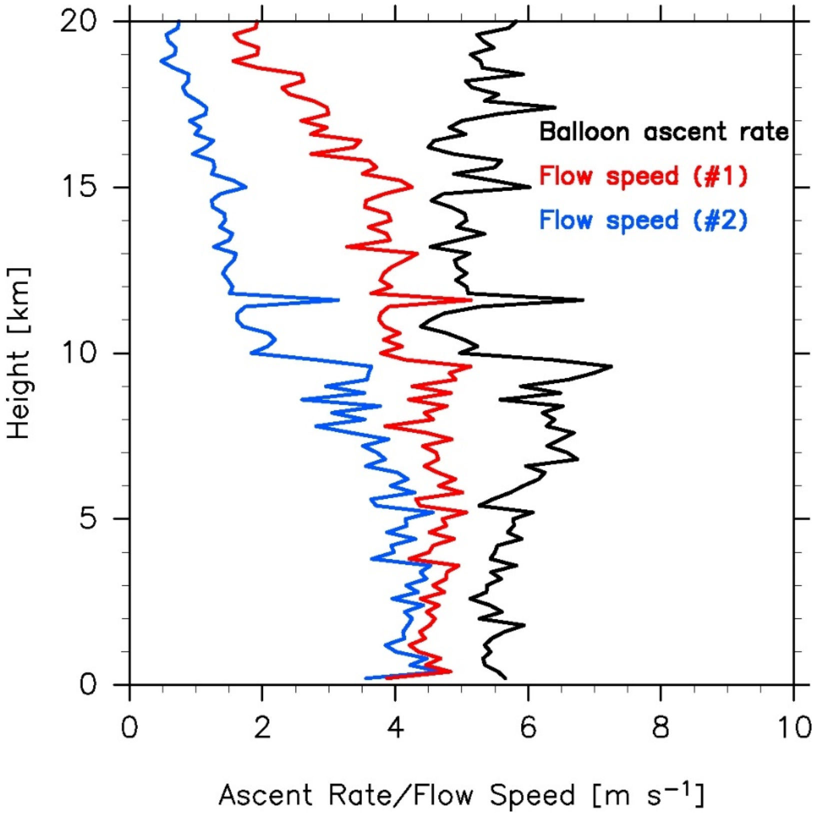

Figure R1-2. Vertical profiles of balloon ascent rate (black) and the flow speed within a duct (with a similar inner cross section to that of the CPS's air inlet) attached to a CPS measured with two hot-wire anemometers, one placed ~4 cm below the detection area (#1, red) and the other ~10 cm below the detection area (#2, blue). Taken at Moriya, Japan, launched at 17:11:47 LT on 23 November 2012. For all three profiles, 0.2-km averages were taken.

The suggestion that the transit time can be used to estimate the particle velocity is not valid. A number of things impact the transit time. If the authors would have shown a frequency histogram of transit times, I think it would show values varying by more than factors of three. The reason is that measuring the transit time from threshold to threshold makes the transit time sensitive to particles size.

In the revised manuscript, we will weaken this suggestion (and point out that selected, high-quality particle signal width data are only useful). The signal width data are primarily used to monitor potential particle overlap in this paper. For the flow speed estimation discussed in Section 2.3, the results from the hot-ware anemometers are primarily referred to; in the revised manuscript, description on the estimation using signal width data will be removed.

Secondly, if the laser used has a Gaussian intensity profile, then the transit time will depend on where *the particle passes through the beam and how far from the center of focus.*

This is true. This is one of the sources of uncertainty in the particle signal width data. However, we do not have quantitative estimates on this at the moment.

Nothing is said about how particles are constrained to go through the most intense portion of the laser beam. What is the sizing error due to passing through edges or away from the center of focus. Laser beams diverge so the scattering intensity from same sized particles can vary widely.

Particles are not constrained to go through a particular point of the detection area. The sizing error due to this treatment is shown in the standard particle experiments described in Appendix A. Let us note here that in Table A3 and Figure A1 of the original manuscript, we incorrectly used values of standard error of the mean (i.e. $\sigma/\sqrt{n}$) rather than standard deviation (σ). We will correct this in the revised manuscript. In Figure R1-3 below, we show the revised Figure A1. The horizontal bars in Figure A1 become much longer (i.e. being multiplied by square root of the number of particles used in each experiment shown in Table A3). The variability in the results, expressed here as the standard deviation, is due to the finite and inhomogeneous detection area and non-constraint particle introduction to it. As seen in this (revised) figure, only a very rough estimate of the particle size is possible with the current CPS1.

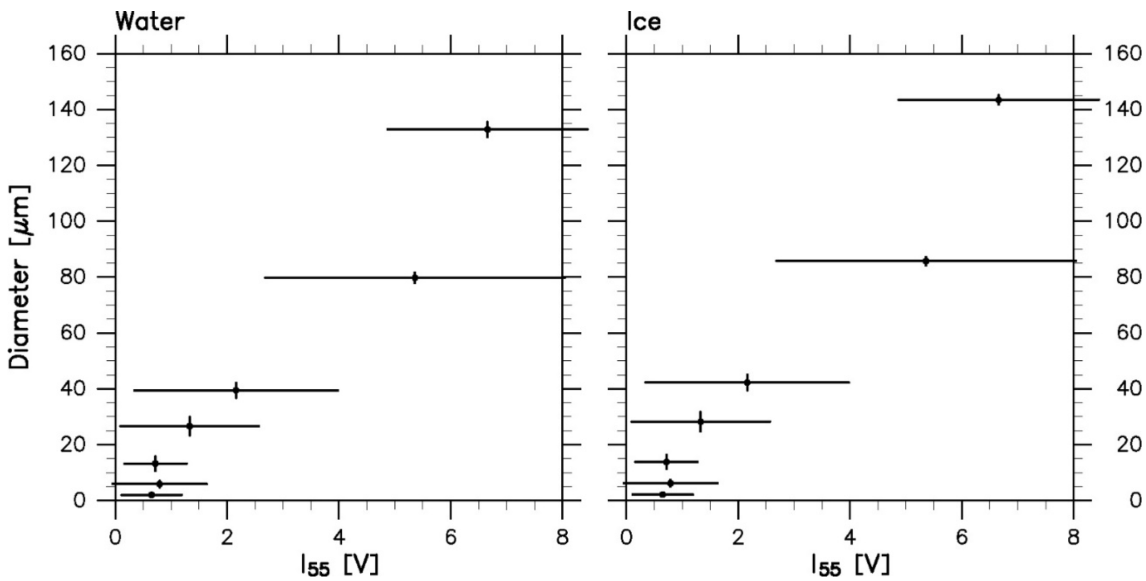

Figure R1-3. Revised Figure A1. (Relationship between I_{55} and the diameters of spherical water droplets (left) and hypothetical spherical ice particles (right) based on Table A2 and the summary column of Table A3. The horizontal bars indicate the standard deviation range obtained from the laboratory experiments, while the vertical bars indicate the minimum and maximum diameters obtained from the Mie scattering calculations.)

Is there a polarized filter in front of the laser to insure linear polarized light? If not, polarized laser diodes, particularly inexpensive ones, will have some fraction of the light in a different plane of polarization. This will bias the signal measured by the polarized detector.

There is no polarized filter in the current version of CPS. The effect of this and other factors (in particular, inhomogeneous laser light intensity within the detection area) results in the DOP distribution (i.e., the one not confined to unity) for spherical and water particles as shown in Figure R1-1 and in the flight results.

How is the sample volume defined? What is the uncertainty in the sample volume? Why use a sample volume that is at last 100 times larger than necessary and limits the concentration due to coincidence? Has this sample volume been mapped out?

Figure R1-4 shows the details of the detection area. As in the figure, the cross section of the detection area that the detectors effectively see is estimated as ~1 cm × 1 cm, while its vertical extent is ~0.5 cm. See above for our priority when we started the development of this instrument.

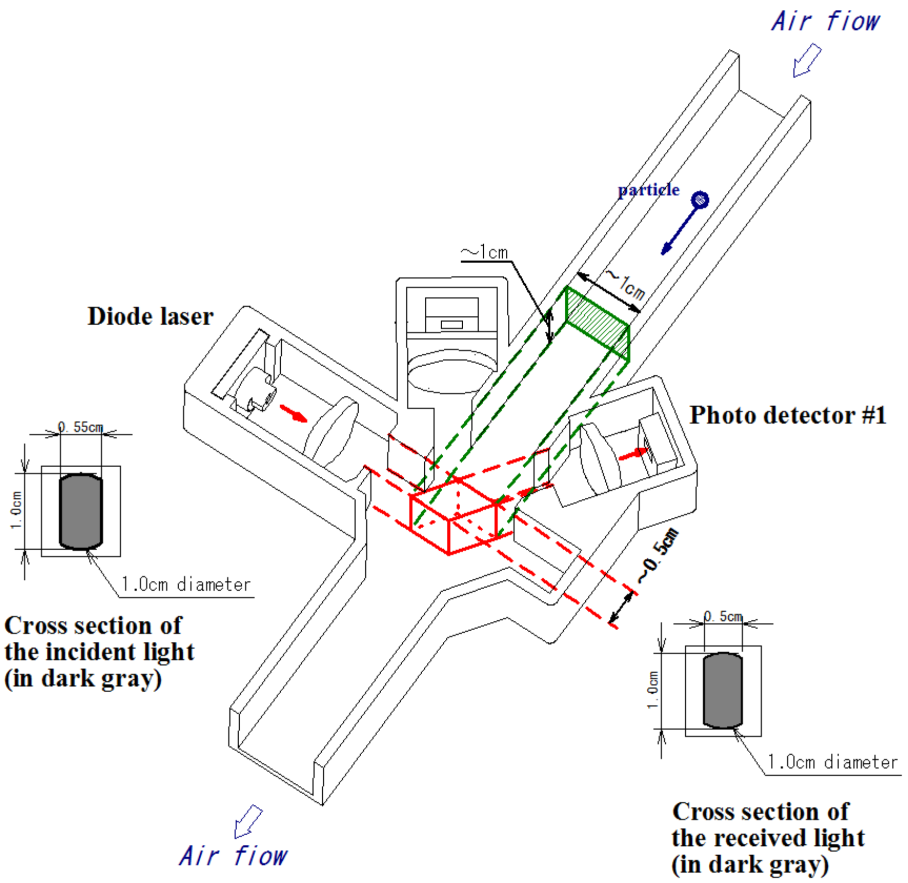

Figure R1-4. Schematic diagram of the CPS, showing the detection area in solid and dotted red lines.

3) Calibration.

"Rough particles" are mentioned as calibration for the polarization channel. What are rough particles?

Please see above.

Where are the calibration curves with water for I125? That would clearly show that there is a size dependent polarization signal for water droplets.

Please see above (the results from the standard spherical particle experiments, in Figure R1-1). Yes, there is some dependence on size as described above, but it is not so large in the 2−100 µm range.

Where is the mapping of the sample volume?

Please see above.

4) Polarization references

There are now a number of instruments that use measurements of the polarization ratio to differentiate spherical from non-spherical particle yet no mention is made of them. This is a significant oversight. There are a number of IN counters that do this, as well as the CAS-POL and CPSPD that differentiate water droplets from ice crystals looking at backscattered, polarized light.

As suggested by Referee #3, in Introduction of the revised manuscript, we will cite the aircraft instruments, the Cloud Aerosol Spectrometer with Polarization (CASPOL; e.g. Nichman et al., 2016), the Small Ice Detector mark 2 (SID-2; e.g. Cotton et al., 2010), and the Cloud Particle Spectrometer with Polarization Detection (CPSPD; Baumgardner et al., 2014). We also cite the article by Baumgardner et al. (2012; see above) and the textbook by Wendisch and Brenguier (2013) for recent developments on the aircraft instruments. Please note, however, that our focus is on developing a balloon-borne instrument flown with a radiosonde, and thus, as discussed in the beginning of this reply, there are several, very different technological issues and emphases. We will also point out that in the lidar community, the polarization information has been used for cloud measurements since the 1970s (Schotland et al., 1971; see also Sassen, 1991).

References:

Baumgardner, D., Newton, R., Krämer, M., Meyer, J., Beyer, A., Wendisch, M., Vochezer, P.: The Cloud Particle Spectrometer with Polarization Detection (CPSPD): A next generation open-path cloud probe for distinguishing liquid cloud droplets from ice crystals, Atmos. Res., 142, 2-14, doi:10.1016/j.atmosres.2013.12.010, 2014.

Cotton, R., Osborne, S., Ulanowski, Z., Hirst, E., Kaye, P. H., and Greenaway, R. S.: The ability of the Small Ice Detector (SID-2) to characterize cloud particle and aerosol morphologies obtained during flights of the FAAM BAe-146 research aircraft, J. Atmos. Oceanic Technol., 27 (2), 290–303, doi: 10.1175/2009JTECHA1282.1, 2010.

Nichman, L., Fuchs, C., Järvinen, E., Ignatius, K., Höppel, N. F., Dias, A., Heinritzi, M., Simon, M., Tröstl, J., Wagner, A. C., Wagner, R., Williamson, C., Yan, C., Connolly, P. J., Dorsey, J. R., Duplissy, J., Ehrhart, S., Frege, C., Gordon, H., Hoyle, C. R., Kristensen, T. B., Steiner, G., McPherson Donahue, N., Flagan, R., Gallagher, M. W., Kirkby, J., Möhler, O., Saathoff, H., Schnaiter, M., Stratmann, F., and Tomé, A.: Phase transition observations and discrimination of small cloud particles by light polarization in expansion chamber experiments, Atmos. Chem. Phys., 16, 3651-3664, doi:10.5194/acp-16-3651-2016, 2016.

Sassen, K.: The polarization lidar technique for cloud research: A review and current assessment, B. Amer. Meteorol. Soc., 72 (12), 1848-1866, doi:10.1175/1520-0477(1991)072<1848:TPLTFC>2.0.CO;2, 1991.

Schotland, R. M., Sassen, K., and Stone, R.: Observations by lidar of linear depolarization ratios for hydrometeors, J. Appl. Meteorol., 10 (5), 1011-1017, doi:10.1175/1520-0450(1971)010<1011:OBLOLD>2.0.CO;2, 1971.

Wendisch, M. and Brenguier, J.-L. (eds): Airborne Measurements for Environmental Research: Methods and Instruments, Wiley-VCH Verlag GmbH & Co. KGaA, Weinheim, Germany, 655 pp., doi:10.1002/97835276532182013, 2013.

In summary, unless the authors can better demonstrate that the CPS will provide any useful cloud property data, this paper should not be accepted for AMT.

Thank you very much again for your comments and suggestions. Please also see the discussion with the other two referees.